

Time-Dependent Superfluid Band Theory for the Inner Crust of Neutron Stars: Current Status and Future Challenges

Kazuyuki Sekizawa^{1,2,3} and Kenta Yoshimura¹

¹ Department of Physics, School of Science, Tokyo Institute of Technology, Tokyo 152-8551, Japan

² Division of Nuclear Physics, Center for Computational Sciences, University of Tsukuba, Ibaraki 305-8577, Japan

³ RIKEN Nishina Center, Saitama 351-0198, Japan
sekizawa@phys.titech.ac.jp, yoshimura.k.ak@m.titech.ac.jp
WWW home page: <https://nuclphystitech.wordpress.com>

Abstract. In this contribution, current status and future prospects of our ongoing project are summarized. In the inner crust of neutron stars, a variety of crystalline structures may emerge, as a result of competition of Coulomb and nuclear interactions, which are immersed in a sea of superfluid neutrons. The best quantum mechanical approach to study properties of dripped neutrons under a periodic potential is the band theory of solids. Concerning the band structure effects on transport properties of neutrons, however, situation is complicated and there has not been established a clear consensus yet. To provide a robust conclusion on the band structure effects, we have developed a fully-microscopic time-dependent band theory based on time-dependent density functional theory (TDDFT), taking full account of Fermionic superfluidity. We have successfully developed a parallel computational code and applied it to the slab phase of nuclear matter. We introduce ongoing works and discuss possible future directions.

Keywords: Neutron stars, inner crust, superfluid, band theory, TDDFT

1 Introduction

One of the ultimate goals of condensed-matter physics would be to predict extremely wide-ranging properties of terrestrial matters based on *ab initio* calculations. Among *ab initio* methods on the market, the density functional theory (DFT) [1] and its time-dependent extension (TDDFT) [2,3] are promising approaches, which have shown great successes in various fields of science, not only condensed-matter physics, but also quantum chemistry and biology, nuclear physics (see, *e.g.*, Refs. [4,5,6,7]), and so forth. In our ongoing project [8,9], we are aiming at revealing properties of *the densest and the largest solids in the universe*—the inner crust of neutron stars—microscopically, applying the band theory of solids [10] based on nuclear (TD)DFT for many-nucleon systems⁴.

⁴ We note that the nuclear (TD)DFT to date is not regarded as an *ab initio* approach.

Table 1. A summary of the situation concerning the band structure effects in the inner crust of neutron stars. An increase of the neutron effective mass ($m_n^*/m_n > 1$), which corresponds to entrainment, is highlighted in red; while the opposite trend ($m_n^*/m_n < 1$), which we call anti-entrainment, is highlighted in blue. In this project, we aim at providing conclusive values of the neutron effective mass throughout the inner crust of neutron stars, based on fully self-consistent superfluid band theory calculations.

Dimension	Self-consistency	Superfluidity	m_n^*/m_n	n_b (fm $^{-3}$)	Ref.
1D	–	–	1.02–1.03	0.074–0.079	
2D	–	–	1.11–1.40	0.058–0.072	[12]
3D	–	–	1.07–15.4	0.03–0.086	[13]
3D	–	–	1.21–13.6	0.0003–0.08	[14]
1D	✓	–	0.65–0.75	0.07–0.08 [†]	[25]
1D	✓	–	0.59	0.04 [‡]	[8]
1D	✓	✓	0.58	0.07 [†]	Our work [9]
2D, 3D	✓	✓	??	$\lesssim 0.07$	Future works

[†] Where appearance of the slab phase is expected.

[‡] With a fixed proton fraction, $Y_p = 0.1$.

In the context of neutron star studies, the band theory may not yet be regarded as a popular or a standard approach. While the structure of nuclear “pasta” in the inner crust of neutron stars may be well described within ordinary DFT calculations (see, *e.g.*, Ref. [11]), transport properties of dripped neutrons may substantially be affected by band structure. It is because of the Bragg scatterings of dripped neutrons off the periodic potential, which are expected to *immobilize* part of dripped neutrons, the so-called *entrainment* effects. In the pioneering works of Refs. [12,13,14], it was shown that the effective mass of dripped neutrons is indeed increased due to the entrainment effects. A notable result was reported for 3D Coulomb lattices at certain baryon number densities ($0.02 \text{ fm}^{-3} \lesssim n_b \lesssim 0.04 \text{ fm}^{-3}$), where the effective mass is predicted to be more than 10 times larger than the bare neutron mass [13,14]. Since such a huge effective mass may potentially affect various interpretations of astrophysical phenomena of neutron stars, *e.g.*, pulsar glitches [15,16,17,18] and thermal as well as crustal properties [19,20,21,22,23], we should pay serious attention to the band structure effects in the inner crust of neutron stars. (See, Ref. [24], for a review of band calculations of Chamel *et al.* and discussion on related topics.)

Recently, fully self-consistent static [25] and dynamic [8] band theories based on nuclear (TD)DFT have been developed and applied for the slab phase of nuclear matter. In Refs. [25,8], it was shown that the neutron effective mass is actually *reduced* by about 30–40%, contrary to the results reported in Ref. [12]. It has thus been highly desired to extend the fully self-consistent band theory for 2D and 3D geometries. One should note that in the aforementioned works pairing correlations (neutron superfluidity) were neglected. While one may estimate effects of pairing with the Bardeen-Cooper-Schrieffer (BCS) approximation [26], on the other hand, a recent work indicates that a self-consistent [Hartree-Fock-Bogoliubov (HFB) type] treatment is essential to correctly quantify the effects of pairing on the entrainment effects [27]. To resolve the arguable situation (see also Table 1), we have recently extended the theoretical framework for super-

fluid systems [9], based on superfluid (TD)DFT with a local treatment of pairing, known as (time-dependent) superfluid local density approximation [(TD)SLDA] [28,29,30]. In this contribution, we provide an overview of our ongoing attempts and discuss future prospects.

The article is organized as follows. In Sec. 2, we briefly summarize the current status of studies with the fully self-consistent band theory for the inner crust of neutron stars. In Sec. 3, we foresee possible future directions and challenges. In Sec. 4, we summarize this contribution.

2 Current Status

2.1 Self-consistent band theory and anti-entrainment effects

The first fully self-consistent band theory calculations based on nuclear DFT were achieved by Kashiwaba and Nakatsukasa in 2019 [25]. In their work, an EDF of the Barcelona-Catania-Paris-Madrid (BCPM) family was employed, whose form is simpler than Skyrme-type EDFs, especially the former does not involve the “microscopic” effective mass ($m_n^{\oplus}/m_n = 1$). In the static band calculations, the “macroscopic” effective mass of dripped neutrons, m_n^* , are defined by⁵

$$m_n^*/m_n = n_n^f/n_n^c, \quad (1)$$

where n_n^f is the free (dripped) neutron number density to which only orbitals with higher single-particle energies than a potential well of the slab contribute. $n_n^c = m_n \mathcal{K}_{zz}$ is the conduction neutron number density, where \mathcal{K}_{zz} is the mobility coefficient which is generally defined as

$$\mathcal{K}_{ij} = 2 \sum_{\nu} \int \frac{d^3k}{(2\pi)^3} \frac{\partial^2 \varepsilon_{\nu\mathbf{k}}^{(n)}}{\partial k_i \partial k_j} \theta(\mu_n - \varepsilon_{\nu\mathbf{k}}^{(n)}). \quad (2)$$

Thus, the contribution from each orbital to the diagonal component such as \mathcal{K}_{zz} is proportional to the curvature of the band. Based on the static treatment, it was shown [25] that the macroscopic effective mass is *smaller* than the bare neutron mass, *i.e.* $m_n^*/m_n = 0.65\text{--}0.75$, contrary to the preceding study [12]⁶.

To further deepen our understanding of the entrainment phenomenon, one of the authors (K.S.) and his collaborators developed a time-dependent version of the self-consistent band theory based on TDDFT [8]. In the latter work, an intuitive, dynamical method to quantify the macroscopic effective mass was proposed. The idea is quite simple. Suppose that we introduce a constant external electric field, which couples only with protons localized inside the slabs, that exerts a constant force, F_{ext} , on protons. Because of the external force, protons and bound as well as entrained neutrons are expected to be dragged. According

⁵ The “microscopic” effective mass refers to the density-dependent one in the EDF, while the “macroscopic” one refers to that associated with the entrainment effects.

⁶ We note that the discrepancy is partly due to an ambiguity in the definition of n_n^f , as discussed in Ref. [25].

to the classical equation of motion, the collective masses of the slab, M_{slab} , and of protons, M_p , (per unit area) can be quantified as

$$M_{\text{slab}}(t) = \dot{P}(t)/a_p(t), \quad M_p(t) = \dot{P}_p(t)/a_p(t), \quad (3)$$

where $a_p(t)$ is the acceleration of center-of-mass position of protons and $P(t)$ is the total linear momentum, $P(t) = P_n(t) + P_p(t)$, with $P_q(t) = \hbar \int j_{z,q}(z, t) dz$. Since we know the collective masses of the slab and of protons, the number density of effectively-bound (bound + entrained) neutrons can be deduced:

$$n_n^{\text{eff. bound}} \equiv (M_{\text{slab}} - M_p)/(am_{n,\text{bg}}^\oplus), \quad (4)$$

where $m_{n,\text{bg}}^\oplus$ is the microscopic effective mass for background neutron number density. Since the conduction neutrons can freely conduct, that is, they are the counter part of the effectively-bound neutrons, there follows

$$n_n^c = \bar{n}_n - n_n^{\text{eff. bound}}, \quad (5)$$

where \bar{n}_n is the average neutron number density. Based on the real-time method, it was shown [8] that the macroscopic effective mass is reduced by 40%, consistent with Ref. [25]. Thanks to the dynamic simulation, it was demonstrated that the reduction is caused by emergence of *counter flow* of dripped neutrons, which flows opposite to the external force. Based on the latter observation, it has been called the *anti-entrainment* effects [8].

2.2 Superfluid extension of the self-consistent band theory

In this section, we provide the essence of the formulation of the fully self-consistent (time-dependent) band theory based on (TD)DFT extended for superfluid systems. We refer readers to Ref. [9] for more detailed descriptions.

As the first step, in Ref. [9], we have formulated the fully self-consistent superfluid band theory for the slab phase of nuclear matter. The key point in formulating the superfluid band theory is to impose the Bloch's boundary condition to the quasiparticle wave functions:

$$u_{\nu\mathbf{k}}^{(q)}(\mathbf{r}\sigma) = \frac{1}{\sqrt{\mathcal{V}}} \tilde{u}_{\nu\mathbf{k}}^{(q)}(z\sigma) e^{i\mathbf{k}\cdot\mathbf{r}}, \quad (6)$$

$$v_{\nu\mathbf{k}}^{(q)}(\mathbf{r}\sigma) = \frac{1}{\sqrt{\mathcal{V}}} \tilde{v}_{\nu\mathbf{k}}^{(q)}(z\sigma) e^{i\mathbf{k}\cdot\mathbf{r}}, \quad (7)$$

where \mathcal{V} denotes the volume of the unit cell, ν is the band index, \mathbf{k} is the Bloch wave vector, q is the isospin ($q = n$ for neutrons, $q = p$ for protons) and σ is the spin ($\sigma = \uparrow$ or \downarrow) of the quasiparticle wave functions. Taking the direction normal to the slabs as z -direction, the lattice translation vector reads $\mathbf{T} = T_x \hat{e}_x + T_y \hat{e}_y + na \hat{e}_z$, where T_x and T_y are arbitrary real numbers, n is an arbitrary integer number, a is the slab period (distance between neighboring slabs), and \hat{e}_i ($i = x, y, z$) is the unit vector along i -direction. The dimensionless

functions, $\tilde{u}_{\nu\mathbf{k}}^{(q)}(z\sigma)$ and $\tilde{v}_{\nu\mathbf{k}}^{(q)}(z\sigma)$, are uniform along x and y directions parallel to the slabs, and manifest the periodicity of the potential, *i.e.*, $\tilde{u}_{\nu\mathbf{k}}^{(q)}(z+na, \sigma) = \tilde{u}_{\nu\mathbf{k}}^{(q)}(z\sigma)$ and $\tilde{v}_{\nu\mathbf{k}}^{(q)}(z+na, \sigma) = \tilde{v}_{\nu\mathbf{k}}^{(q)}(z\sigma)$.

By substituting the quasiparticle wave functions (6) and (7) into the SLDA equation, which is formally similar to the so-called Hartree-Fock-Bogoliubov (HFB) or Bogoliubov-de Gennes (BdG) equation, we find [9]:

$$\begin{pmatrix} \hat{h}^{(q)} + \hat{h}_{\mathbf{k}}^{(q)} - \lambda_q & \Delta_q(z) \\ \Delta_q^*(z) & -\hat{h}^{(q)*} - \hat{h}_{-\mathbf{k}}^{(q)*} + \lambda_q \end{pmatrix} \begin{pmatrix} \tilde{u}_{\nu\mathbf{k}}^{(q)}(z\uparrow) \\ \tilde{v}_{\nu\mathbf{k}}^{(q)}(z\downarrow) \end{pmatrix} = E_{\nu\mathbf{k}} \begin{pmatrix} \tilde{u}_{\nu\mathbf{k}}^{(q)}(z\uparrow) \\ \tilde{v}_{\nu\mathbf{k}}^{(q)}(z\downarrow) \end{pmatrix}, \quad (8)$$

where λ_q is the chemical potential for neutrons $q = n$ and for protons $q = p$. $\hat{h}^{(q)}(z)$ and $\Delta_q(z)$ are the single-particle Hamiltonian and the pairing field, respectively, which can be derived from appropriate functional derivatives of an energy density functional (EDF). In this work, we have developed the formalism with a widely-used Skyrme-type EDF. The \mathbf{k} -dependent single-particle Hamiltonian is defined by

$$\hat{h}_{\mathbf{k}}^{(q)}(z) = \frac{\hbar^2 \mathbf{k}^2}{2m_q^\oplus(z)} + \hbar \mathbf{k} \cdot \hat{\mathbf{v}}^{(q)}(z), \quad (9)$$

where $\hat{\mathbf{v}}^{(q)}(z)$ is the so-called velocity operator, $\hat{\mathbf{v}}^{(q)}(z) = [\mathbf{r}, \hat{h}^{(q)}(z)]/(i\hbar)$. The \mathbf{k} -dependent term emerges, because of an operation of spatial derivatives on the Bloch factor $e^{i\mathbf{k}\cdot\mathbf{r}}$ in the quasiparticle wave functions (6) and (7). For the dynamic calculations, we work with the TDSLDA equation in the velocity gauge [8]. In Ref. [9], we have found that the neutron superfluidity affects little on the entrainment effects, at least for the slab phase of nuclear matter.

3 Future Directions and Challenges

3.1 Extensions to finite temperatures

The extension to finite temperatures can be achieved in a straightforward way. In (TD)SLDA, finite-temperature effects can be incorporated by modifying the formulas of various densities [28]. For the number density, for instance, it reads:

$$n_q(\mathbf{r}, t) = \sum_{E_\mu > 0} \sum_{\sigma} \left[f(-E_\mu) |v_\mu^{(q)}(\mathbf{r}\sigma, t)|^2 + f(E_\mu) |u_\mu^{(q)}(\mathbf{r}\sigma, t)|^2 \right], \quad (10)$$

and similar modifications are applied for other densities as well. The function $f(E)$ is defined as $f(E) = [1 + \exp(\beta E)]^{-1}$ with the inverse temperature, $\beta = 1/(k_B T)$, where k_B is the Boltzmann constant. In the superfluid band theory calculations, the quasiparticle states in the summation, μ , becomes a combination of quasiparticle states and Bloch wave vectors, $\mu \rightarrow \{\nu, \mathbf{k}\}$.

In Fig. 1, we show a result of exploratory calculations for $n_b = 0.05 \text{ fm}^{-3}$ in the β equilibrium within the period $a = 30 \text{ fm}$. In panels (a–d), neutron and proton density distributions are shown as a function of z coordinate. From

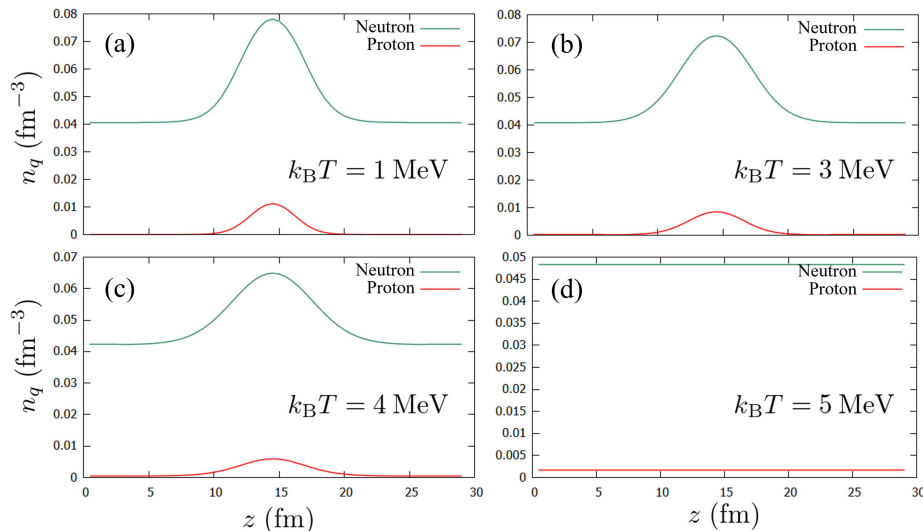


Fig. 1. Neutron (green) and proton (red) density distributions are shown as a function of z coordinate. In panels (a–d), results of self-consistent band theory calculations are shown at $k_B T = 1, 3, 4,$ and 5 MeV, respectively.

panels (a) to (d), temperature corresponds to $k_B T = 1, 3, 4,$ and 5 MeV, respectively. From the figure, it is visible that the slab shape becomes more diffusive as temperature increases. We note that the neutron superfluidity has already gone at $k_B T \simeq 0.8$ MeV. At $k_B T = 5$ MeV, the system eventually becomes uniform, indicating that the nuclear slab has melted. We aim to predict how nuclear pasta may have been “cooked” during/after a supernova explosion or a neutron-star merger, based on microscopic band theory calculations. Besides, following the formalism of Ref. [31], we can now calculate the elastic and inelastic static structure factors for the slab phase of nuclear matter within the superfluid band theory at finite temperatures [32]. With the latter quantities we can evaluate neutrino-pasta scattering cross sections and, thus, the neutrino opacity, which could be an important input for simulations of a supernova explosion or cooling of a proto-neutron star.

3.2 Extension to finite magnetic fields

We can also include finite magnetic-field effects into the description. The leading effects of a magnetic field comes from the Landau-Rabi quantization of relativistic electron gas. Because of the formation of Landau levels, the electron fraction is enhanced, which also enhances the proton fraction through the charge neutrality condition. In this way, the magnetic field can directly alter the composition of (n, p, e) matter and affects the structure of the crusts (see, *e.g.*, Ref. [33], and references therein).

The magnetic field can also interact with nucleons through the magnetic moments. On one hand, however, we know that a really strong magnetic field, as large as $B \gtrsim 10^{17}$ G, is required to affect the nuclear structure (see, *e.g.*,

Refs. [34,35]). It is simply because of the fact that such a strong magnetic field is necessary to make the energy shifts caused by a magnetic field on the order of MeV. Thus, the outer crust of the majority of neutron stars (with $B \simeq 10^{12}$ – 10^{13} G or, at most, $\approx 10^{16}$ G in strongly-magnetized magnetars) magnetic field effects on nuclear structure could safely be neglected. On the other hand, in the inner crust of neutron stars, dripped neutrons exhibit complex band structure, where band gaps can be much smaller than 1 MeV. It may be possible that a magnetic field alters the band structure even for a smaller magnetic-field strength ($\lesssim 10^{14}$ – 10^{15} G). Thus, we are going to explore possible effects of a magnetic field on crustal and/or transport properties of dripped neutrons in the inner crust of neutron stars.

The extension to include the finite magnetic-field effects are in progress. By allowing *spin polarization* of neutrons and protons within the asymmetric SLDA (ASLDA) framework [28,36], we plan to investigate spin polarization of nuclear matter under a superstrong magnetic field in a fully microscopic framework. At the same time, it would be interesting to explore possible emergence of the *spin-triplet* pairing under such an extreme condition (*cf.* Ref. [37]). We consider that it is possible to extend our framework to describe the spin-triplet pairing by introducing the spin-current pair density, as recently discussed in Ref. [38].

3.3 Extension to higher spatial dimensions

We anticipate that the extension to higher spatial dimensions (*i.e.*, 2D and 3D geometries) is not only straightforward, but also many knowledges and techniques can be brought from the ordinary band theory for terrestrial solids in condensed-matter physics. We thus consider that the main obstacle to achieve this extension will be the computational cost. For the slab phase (a 1D crystal) with a typical numerical setup for actual simulations (with $\Delta z = 0.5$ fm, $a \simeq 30$ fm), the number of quasiparticle wave functions is estimated to be 2,880,000 [9]. That is, we have already dealt with time evolution of *millions* of quasiparticle wave functions by solving complex, non-linear, coupled partial differential equations (PDEs). Even though the computational cost per quasiparticle wave function is rather small for the 1D system, we have implemented the MPI parallelization for k_z to reduce actual computation time.

For the rod phase (a 2D crystal), for instance, taking the direction of rod-shaped nuclear clusters along z direction, the number of quasiparticle wave functions becomes $N_x \times N_y \times N_{k_x} \times N_{k_y} \times N_{k_{\parallel}} \times 2$ (n and p) $\times 2$ (u and v), where k_{\parallel} represents the Bloch wave number along the rods. We may, in this case, increase the lattice spacing to $\Delta z = 1.0$ or 1.2 fm, leading to $N_x \times N_y \simeq 625$ – 900 , assuming the area of a unit cell is roughly 30^2 fm². Those lattice spacings are often used for nuclear (TD)DFT calculations. By roughly estimating $N_{k_x} \times N_{k_y} \times N_{k_{\parallel}} \approx 80^3$, the total number of quasiparticle wave functions already exceeds 1 billion!

We note that the estimated numbers of quasiparticle wave functions will be doubled, if we introduce an interaction that mixes spin states (*e.g.*, the spin-orbit interaction) or an external field that breaks the time-reversal symmetry (*e.g.*, a magnetic field). Although one could reduce significantly the number of

quasiparticle wave functions by employing an EDF that does not involve the microscopic (density-dependent) effective mass (*i.e.*, $m_n^\oplus/m_n = 1$), as was employed in Ref. [25], we are facing a computational challenge to solve an enormous number of complex, non-linear, coupled PDEs for time evolution of quasiparticle wave functions to simulate dynamics of neutron star crustal matter within a fully self-consistent superfluid band theory. We plan to use the GPGPU parallelization, successfully employed in Refs. [30,39], to attack the problem.

4 Summary

In this project, we aim at establishing a microscopic, fully self-consistent time-dependent band theory taking into account various effects such as superfluidity, finite temperatures and magnetic fields, and so on. We have just put forward the first step towards this goal in Ref. [9]. We note that the present formalism can be used for a unified description of a neutron star, although the band structure effects are absent in the outer crust and core regions. If the project completes successfully, it will provide us a fully microscopic equation of states (EoS) with effects of band structure and neutron superfluidity as well as proton superconductivity at arbitrary temperatures and magnetic fields, which will be the most reliable class of EoS on the market that can be used for a variety of applications such as simulations of supernova explosions or neutron star mergers. The next step, the finite-temperature extension, will be published elsewhere [32].

Acknowledgments. Meetings in the A3 Foresight Program supported by JSPS are acknowledged for useful discussions. One of the authors (K.Y.) would like to acknowledge the support from the Hiki Foundation, Tokyo Institute of Technology. This work mainly used computational resources of the Yukawa-21 supercomputer at Yukawa Institute for Theoretical Physics (YITP), Kyoto University. This work also used (in part) computational resources of the HPCI system (Grand Chariot) provided by Information Initiative Center (IIC), Hokkaido University, through the HPCI System Project (Project ID: hp230180). This work is supported by JSPS Grant-in-Aid for Scientific Research, Grant Nos. 23K03410 and 23H01167.

References

1. Kohn, W.: Nobel Lecture: Electronic structure of matter—wave functions and density functionals, *Rev. Mod. Phys.* **71**, 1253 (1999). doi.org/10.1103/RevModPhys.71.1253
2. Marques, M.A.L., Ullrich, C.A., Nogueira, F., Rubio, A., Burke, K., Gross, E.K.U.: *Time-Dependent Density Functional Theory*, *Lect. Notes Phys.* **706** (Springer Berlin, Heidelberg, 2006). doi.org/10.1007/b11767107
3. Marques, M.A.L., Maitra, N.T., Nogueira, F.M.S., Gross, E.K.U.: *Fundamentals of Time-Dependent Density Functional Theory*, (ed.) A. Rubio, *Lect. Notes in Phys.*, Vol. **837** (Springer Berlin, Heidelberg, 2012). doi.org/10.1007/978-3-642-23518-4
4. Bender, M., Heenen, P.-H., Reinhard, P.-G.: Self-consistent mean-field models for nuclear structure, *Rev. Mod. Phys.* **75**, 121 (2003). doi.org/10.1103/RevModPhys.75.121

5. Nakatsukasa, T., Matsuyanagi, K., Matsuo, M., Yabana, K.: Time-dependent density-functional description of nuclear dynamics, *Rev. Mod. Phys.* **88**, 045004 (2016). doi.org/10.1103/RevModPhys.88.045004
6. Sekizawa, K.: TDHF Theory and Its Extensions for the Multinucleon Transfer Reactions: a Mini Review, *Front. Phys.* **7**, 20 (2019). doi.org/10.3389/fphy.2019.00020
7. Coló, G.: Nuclear density functional theory, *Advances in Physics: X*, **5**, 1740061 (2020). doi.org/10.1080/23746149.2020.1740061
8. Sekizawa, K., Kobayashi, S., Matsuo, M.: Time-dependent extension of the self-consistent band theory for neutron star matter: Anti-entrainment effects in the slab phase, *Phys. Rev. C* **105**, 045807 (2022). doi.org/10.1103/PhysRevC.105.045807
9. Yoshimura, K., Sekizawa, K.: Superfluid extension of the self-consistent time-dependent band theory for neutron star matter: Anti-entrainment vs. superfluid effects in the slab phase, arXiv:2306.03327 [nucl-th]. doi.org/10.48550/arXiv.2306.03327
10. Ashcroft, N.W., Mermin, N.D., Wei, D.: *Solid State Physics Revised Edition* (Cengage Learning Asia Pte Ltd, 2016).
11. Schuettrumpf, B., Martínez-Pinedo, G., Afibuzzaman, Md., Aktulga, H.M.: Survey of nuclear pasta in the intermediate-density regime: Shapes and energies, *Phys. Rev. C* **100**, 045806 (2019). doi.org/10.1103/PhysRevC.100.045806
12. Carter, B., Chamel, N., Haensel, P.: Entrainment coefficient and effective mass for conduction neutrons in neutron star crust: simple microscopic models, *Nucl. Phys. A* **748**, 675 (2005). doi.org/10.1016/j.nuclphysa.2004.11.006
13. Chamel, N.: Band structure effects for dripped neutrons in neutron star crust, *Nucl. Phys. A* **747**, 109 (2005). doi.org/10.1016/j.nuclphysa.2004.09.011
14. Chamel, N.: Neutron conduction in the inner crust of a neutron star in the framework of the band theory of solids, *Phys. Rev. C* **85**, 035801 (2012). doi.org/10.1103/PhysRevC.85.035801
15. Andersson, N., Glampedakis, K., Ho, W.C.G., Espinoza, C.M.: Pulsar Glitches: The Crust is not Enough, *Phys. Rev. Lett.* **109**, 241103 (2012). doi.org/10.1103/PhysRevLett.109.241103
16. Chamel, N.: Crustal Entrainment and Pulsar Glitches, *Phys. Rev. Lett.* **110**, 011101 (2013). doi.org/10.1103/PhysRevLett.110.011101
17. Haskell, B., Melatos, A.: Models of pulsar glitches, *Int. J. Mod. Phys. D* **24**, 1530008 (2015). doi.org/10.1142/S0218271815300086
18. Watanabe, G., Pethick, C.J.: Superfluid Density of Neutrons in the Inner Crust of Neutron Stars: New Life for Pulsar Glitch Models, *Phys. Rev. Lett.* **119**, 062701 (2017). doi.org/10.1103/PhysRevLett.119.062701
19. Chamel, N., Margueron, J., Khan, E.: Neutron specific heat in the crust of neutron stars from the nuclear band theory, *Phys. Rev. C* **79**, 012801(R) (2009). doi.org/10.1103/PhysRevC.79.012801
20. Chamel, N., Page, D., Reddy, S.: Low-energy collective excitations in the neutron star inner crust, *Phys. Rev. C* **87**, 035803 (2013). doi.org/10.1103/PhysRevC.87.035803
21. Kobyakov, K., Pethick, C.J.: Dynamics of the inner crust of neutron stars: Hydrodynamics, elasticity, and collective modes, *Phys. Rev. C* **87**, 055803 (2013). doi.org/10.1103/PhysRevC.87.055803
22. Kobyakov, K., Pethick, C.J.: Nucleus-nucleus interactions in the inner crust of neutron stars, *Phys. Rev. C* **94**, 055806 (2016). doi.org/10.1103/PhysRevC.94.055806
23. Durel, D., Urban, M.: Long-wavelength phonons in the crystalline and pasta phases of neutron-star crusts, *Phys. Rev. C* **97**, 065805 (2018). doi.org/10.1103/PhysRevC.97.065805

24. Chamel, N.: Entrainment in Superfluid Neutron-Star Crusts: Hydrodynamic Description and Microscopic Origin, *J. Low Temp. Phys.* **189**, 328 (2017). doi.org/10.1007/s10909-017-1815-x
25. Kashiwaba, Yu, Nakatsukasa, T.: Self-consistent band calculation of the slab phase in the neutron-star crust, *Phys. Rev. C* **100**, 035804 (2019). doi.org/10.1103/PhysRevC.100.035804
26. Carter, B., Chamel, N., Haensel, P.: Effect of BCS pairing on entrainment in neutron superfluid current in neutron star crust, *Nucl. Phys.* **A759**, 441 (2005). doi.org/10.1016/j.nuclphysa.2005.05.151
27. Minami, Y., Watanabe, G.: Effects of pairing gap and band gap on superfluid density in the inner crust of neutron stars, *Phys. Rev. Research* **4**, 033141 (2022). doi.org/10.1103/PhysRevResearch.4.033141
28. Bulgac, A., Forbes, M.M., Magierski, P.: *The Unitary Fermi Gas: From Monte Carlo to density functionals*, in *BCS-BEC Crossover and the Unitary Fermi Gas*, (ed.) W. Zwerger, *Lect. Notes Phys.* (Springer, Berlin, Heidelberg, 2012), Vol. **836**, pp. 305–373. doi.org/10.1007/978-3-642-21978-8_9
29. Bulgac, A.: Time-Dependent Density Functional Theory for Fermionic Superfluids: From Cold Atomic Gases–To Nuclei and Neutron Stars Crust, *Phys. Status Solidi B* **256**, 1800592 (2019). doi.org/10.1002/pssb.201800592
30. Jin, S., Roche, K.J., Stetcu, I., Abdurrahman, I., Bulgac, A.: The LISE package: Solvers for static and time-dependent superfluid local density approximation equations in three dimensions, *Comput. Phys. Commun.* **269**, 108130 (2021). doi.org/10.1016/j.cpc.2021.108130
31. Schuetrumpf, B., Martínez-Pinedo, G., Reinhard, P.-G.: Survey of nuclear pasta in the intermediate-density regime: Structure functions for neutrino scattering, *Phys. Rev. C* **101**, 055804 (2020). doi.org/10.1103/PhysRevC.101.055804
32. K. Yoshimura and K. Sekizawa, in preparation.
33. Sekizawa, K., Kaba, K.: Possible Existence of Extremely Neutron-Rich Superheavy Nuclei in Neutron Star Crusts Under a Superstrong Magnetic Field, arXiv:2302.07923 [nucl-th]. doi.org/10.48550/arXiv.2302.07923
34. Peña Arteaga, D., Grasso, M., Khan, E., Ring, P.: Nuclear structure in strong magnetic fields: Nuclei in the crust of a magnetar, *Phys. Rev. C* **84**, 045806 (2011). doi.org/10.1103/PhysRevC.84.045806
35. Stein, M., Maruhn, J., Sedrakian, A., Reinhard, P.-G.: Carbon-oxygen-neon mass nuclei in superstrong magnetic fields, *Phys. Rev. C* **94**, 035802 (2016). doi.org/10.1103/PhysRevC.94.035802
36. Tüzemen, B., Zawiślak, T., Wlazłowski, G., Magierski, P.: Disordered structures in ultracold spin-imbalanced Fermi gas, *New J. Phys.* **25**, 033013 (2023). doi.org/10.1088/1367-2630/acc26b
37. Tajima, H., Funaki, H., Sekino, Y., Yasutake, N., Matsuo, M.: Exploring 3P_0 Superfluid in Dilute Spin-Polarized Neutron Matter, arXiv:2305.08690 [nucl-th]. doi.org/10.48550/arXiv.2305.08690
38. Hinohara, N., Oishi, T., Yoshida, K.: Triplet-odd pairing in finite nuclear systems (I): Even-even singly-closed nuclei, arXiv:2308.02617 [nucl-th]. doi.org/10.48550/arXiv.2308.02617
39. Jin, S., Bulgac, A., Roche, K., Wlazłowski, G.: Coordinate-space solver for superfluid many-fermion systems with the shifted conjugate-orthogonal conjugate-gradient method, *Phys. Rev. C* **95**, 044302 (2017). doi.org/10.1103/PhysRevC.95.044302